

# In vivo therapeutic effect of CDH3/P-cadherin-targeting radioimmunotherapy

Hiroki Yoshioka · Shinji Yamamoto · Hirofumi Hanaoka · Yasuhiko Iida · Pramila Paudyal · Tetsuya Higuchi · Hideyuki Tominaga · Noboru Oriuchi · Hidewaki Nakagawa · Yasuhiro Shiba · Koji Yoshida · Ryuji Osawa · Toyomasa Katagiri · Takuya Tsunoda · Yusuke Nakamura · Keigo Endo

Received: 22 September 2011 / Accepted: 7 December 2011 / Published online: 6 January 2012  
© Springer-Verlag 2012

## Abstract

**Purpose** We examined the possible efficacy of the yttrium-90 (<sup>90</sup>Y)-labeled anti-CDH3/P-cadherin mouse monoclonal antibody (MAB-6) in radioimmunotherapy (RIT) for lung and colorectal cancers that express CDH3/P-cadherin.

**Experimental design** MAB-6 was established using genetic immunization. The biodistribution of MAB-6 in nude mice with lung and colorectal cancers was examined by administering indium-111(<sup>111</sup>In)-labeled MAB-6 to mice. The mice were prepared by inoculation of CDH3/P-cadherin-positive (EBC1, H1373, and SW948) and CDH3/P-cadherin-negative (A549 and RKO) tumor cells. Therapeutic effects and toxicity were investigated by administration of <sup>90</sup>Y-labeled MAB-6 (<sup>90</sup>Y-MAB-6) to EBC, H1373, and SW948-inoculated mice.

**Results** Our in vivo results confirmed the specific binding of MAB-6 to tumor cells after intravenous injections of <sup>111</sup>In-labeled MAB-6 to mice with tumors expressing CDH3/P-cadherin. A single intravenous injection of <sup>90</sup>Y-MAB-6 (100 μCi) significantly suppressed tumor growth in mice with tumors expressing CDH3/P-cadherin. Furthermore, two injections of <sup>90</sup>Y-MAB-6 led to complete tumor regression in H1373-inoculated mice without any detectable toxicity.

**Conclusions** Our findings demonstrate that CDH3/P-cadherin-targeting RIT with <sup>90</sup>Y-MAB-6 is a promising strategy for the treatment for cancers expressing CDH3/P-cadherin.

**Keywords** Radioimmunotherapy · CDH3/P-cadherin · Xenograft · Lung cancer · Colorectal cancer

**Electronic supplementary material** The online version of this article (doi:10.1007/s00262-011-1186-0) contains supplementary material, which is available to authorized users.

H. Yoshioka (✉) · S. Yamamoto · P. Paudyal · T. Higuchi · H. Tominaga · N. Oriuchi · K. Endo  
Department of Diagnosis of Radiology and Nuclear Medicine,  
Gunma University Graduate School of Medicine,  
3-39-22, Showa-machi, Maebashi, Gunma 371-8511, Japan  
e-mail: h-yoshioka@oncotherapy.co.jp

H. Yoshioka · S. Yamamoto · Y. Shiba · K. Yoshida · R. Osawa · T. Katagiri · T. Tsunoda  
Oncotherapy Science Inc., Kanagawa Science Park R&D D6F,  
3-2-1 Sakado, Takatsu-ku, Kawasaki,  
Kanagawa 213-0012, Japan

H. Hanaoka · Y. Iida · K. Endo  
Department of Bioimaging Information Analysis,  
Gunma University Graduate School of Medicine,  
3-39-22, Showa-machi, Maebashi, Gunma 371-8511, Japan

H. Nakagawa  
Laboratory of Biomarker Development,  
Center for Genomic Medicine, RIKEN, 4-6-1, Shirokanedai,  
Minato-ku, Tokyo 108-0071, Japan

T. Katagiri  
Division of Genome Medicine, Institute for Genome Research,  
The University of Tokushima, 3-18-15, Kuramoto-cyuo,  
Tokushima 770-8503, Japan

Y. Nakamura  
Laboratory of Molecular Medicine, Human Genome Center,  
Institute of Medical Science, The University of Tokyo,  
4-6-1 Shirokanedai, Minato-ku, Tokyo 108-8639, Japan

## Introduction

The administration of monoclonal antibodies (mAbs) against cell-surface molecules is one of the key treatment strategies for various cancers. The recent clinical successes of anticancer antibodies such as rituximab (Rituxan) [1], trastuzumab (Herceptin) [2], bevacizumab (Avastin) [3], and cetuximab (Erbix) [4] have improved antibody-based therapeutics for solid tumors and hematopoietic malignancies. The antitumor effects of mAbs are considered to be enhanced by their use in combination with other treatment methods (e.g., radiotherapy or chemotherapy). In particular, radiolabeling of mAbs has the advantage of an intrinsic “cross-fire” effect that may overcome the heterogeneous expression of cancer cells with regard to molecular target expression [5–7]. For example, ibritumomab tiuxetan (Zevalin), which is a yttrium-90 ( $^{90}\text{Y}$ )-conjugated anti-CD20 antibody, has been approved for patients with relapsed or refractory low-grade follicular or transformed B-cell non-Hodgkin’s lymphoma (NHL) and those with follicular B-cell NHL that is refractory to rituximab (Rituxan) therapy [8, 9]. Although these results are promising when compared to responses of advanced cancers to current cytotoxic anticancer drugs, the proportion of patients showing a good response is limited; moreover, in some patients, the adverse reactions caused by these chemotherapies are severe. Therefore, it is important to develop new therapeutic antibodies targeting cancer-specific molecules on the cell surfaces.

In order to develop novel agents that improve cancer treatment, we have previously analyzed the gene expression profiles of various cancers by means of a genome-wide expression profile analysis [10–14]. Subsequently, we identified CDH3/P-cadherin as a promising molecular target in the development of a novel anticancer therapy. Considerable upregulation of CDH3/P-cadherin at the protein level has been confirmed in pancreatic, gastric, and colorectal cancers [15]. Furthermore, in this study, the expression of CDH3/P-cadherin in lung and bladder cancers has been confirmed to be upregulated and very high, whereas that in normal organs, except in the esophagus, is absent or very low.

CDH3/P-cadherin is a single-span transmembrane glycoprotein that mediates the adhesion, proliferation, and invasion of tumor cells [16]. Using small interfering RNA, we have previously experimentally demonstrated that CDH3/P-cadherin is involved in the growth of pancreatic cancer cells and that the antibody against CDH3/P-cadherin inhibits the motility of cancer cells *in vitro* [17].

Therefore, in this study, we explored the therapeutic potential of targeting CDH3/P-cadherin-positive tumor cells via RIT. We generated a mouse monoclonal antibody (MAb-6) by genetic immunization that specifically bound to CDH3/P-cadherin. We also demonstrated its promising

therapeutic effects by its conjugation to  $^{90}\text{Y}$  on xenograft tumors in nude mice without any detectable adverse effects.

## Materials and methods

### Cells

The cancer cell lines A549 and NCI-H1373 (derived from lung adenocarcinoma; hereafter referred to as H1373), EBC1 (derived from squamous cell carcinoma of the lung), RKO, and SW948 (derived from colorectal carcinoma) were used in this study. A549, H1373, RKO, and SW948 cell lines were purchased from American Type Culture Collection (Manassas, VA, USA) and EBC1 cell line, from the Japan Cancer Research Resources Bank (Tokyo, Japan). Cell lines were cultured under their respective depositors’ recommendation (RPMI 1640 for A549 and H1373 cell lines; EMEM for RKO cell line; and Leibovitz’s L-15 medium for SW948 cell line) and maintained in growth medium supplemented with 10% fetal bovine serum and penicillin/streptomycin at 37°C in a humidified atmosphere of 5%  $\text{CO}_2$  (except SW948 cells, which were maintained in a  $\text{CO}_2$ -free environment).

### Antibodies

MAb-6 was generated by immunizing mice with an expression vector designed to express a partial protein of CDH3 corresponding to an extracellular domain (Norsan Corporation, Yokohama, Japan) [18]. For immunohistochemical (IHC) analysis and western blotting, anti-CDH3, anti-CDH1, and anti-CDH2 mouse mAbs were purchased from BD Transduction Laboratories (San Jose, CA, USA).  $\beta$ -Actin (ACTB) mouse monoclonal antibody was purchased from Biovision (Mountain View, CA, USA). A non-specific control antibody, mouse IgG1, was purchased from Beckman Coulter (Fullerton, CA, USA). For animal studies, another control antibody, mouse IgG1, was purchased from Nordic Immunological Laboratories (Tilburg, The Netherlands) in a medium that did not contain sodium azide.

### Western blotting

Cells were lysed by RIPA buffer containing 50 mmol/l (pH 8.0) Tris, 150 mmol/l NaCl, 1.0% NP-40, and 0.5% sodium deoxycholate and phenylmethylsulfonyl fluoride. The protein concentration of each lysate was determined by the Bio-Rad Protein Assay Kit (Bio-Rad, Hercules, CA, USA) with bovine serum albumin (BSA) as a standard. Lysates (30  $\mu\text{g}$  each) were separated on 7.5% denaturing polyacrylamide gels and transferred electrophoretically to polyvinylidene fluoride membranes (Millipore, Billerica, MA, USA).

After blocking with 4% Blockase (DS Pharma Biomedical, Osaka, Japan), membranes were incubated with primary antibodies for 1 h at room temperature. Immunoreactive proteins were detected by incubation with horseradish peroxidase-conjugated secondary antibodies (KPL, Gaithersburg, MD, USA) for 1 h at room temperature. After washing with TBS (tris-buffered saline) with 0.05% Tween 20, the membrane was developed using Immobilon Western (Millipore). After development, films were scanned and images saved using ImageJ software (Java-based image processing software). A region of interest was drawn over the first lane and was applied to other lanes as well as the background to obtain densitometric signals from an equal area. The value of CDH3 intensity was normalized to that of ACTB.

#### Flow cytometry

Cells were harvested using cell dissociation buffer (Gibco BRL, Rockville, MD, USA). A suspension of  $1 \times 10^6$  cells was incubated with 50  $\mu\text{g}/\text{ml}$  of MAb-6 or non-immunized mouse control IgG for 1 h at 4°C. After washing with 0.5% BSA in PBS(-), 2 mg/ml Alexa Fluor 488-goat anti-mouse IgG (Invitrogen, Carlsbad, CA, USA) containing 2.5  $\mu\text{g}/\text{ml}$  of 7-AAD (7-amino-actinomycin D; Beckman Coulter) was added, and cell suspensions were incubated for 30 min at 4°C and were analyzed using FACScan (Becton–Dickinson, Franklin Lakes, NJ, USA).

#### Preparation of human and mouse cell lines stably expressing CDH3

cDNA encoding the open reading frame of CDH3 was amplified by polymerase chain reaction (PCR) using primers incorporating restriction enzyme sites (shown underlined below): human CDH3 [5'-CCGGAATTCGCCACC ATGGGGCTCCCTCGTGGACC-3' (forward) and 5'-ACG CGTCGACGTCGTCTCCCGCCACCGT-3' (reverse)]; mouse CDH3 [5'-CCGGAATTCGCCACCATGGAGCTT CTTAGTGGGCCT-3' (forward) and 5'-ACGCGTCGAC GTCATCCTCACC GCCACCATAC-3' (reverse)]. The PCR products were cloned into a pCAGGS-neo vector. The plasmids were transfected into A549 cells, in which undetectable CDH3 expression was observed, using FuGENE 6 (Roche, Basel, Switzerland) according to the manufacturer's instructions. After transfection, cells were selected with 0.8 mg/ml of geneticin (Invitrogen). The Mock vector pCAGGS-neo vector was transfected as the control. After limiting the dilution for screening, some colonies were selected. The expression of transfected genes in the clones was evaluated by western blotting with anti-Flag antibodies (Sigma Aldrich, St. Louis, MO, USA). Three FLAG-human CDH3 and FLAG-mouse clones stably overexpressing CDH3 were established and used for experimentation.

#### Radiolabeling of antibody–chelator conjugates

Antibodies were labeled with indium-111 ( $^{111}\text{In}$ ; Nihon Medi-Physics, Hyogo, Japan) for biodistribution studies and with  $^{90}\text{Y}$  (Eckert & Ziegler Nuclitec, Braunschweig, Germany) for therapeutic studies [19, 20]. Antibody labeling with  $^{111}\text{In}$  and  $^{90}\text{Y}$  was achieved via a bifunctional metal ion-chelating agent *p*-isothiocyanatobenzyl diethylenetriaminepentaacetic acid (*p*-SCN-Bz-DTPA; Macrocyclics, Dallas, TX, USA). Antibodies in 50 mM borate buffer (pH 8.5) were conjugated to *p*-SCN-Bz-DTPA in dimethylformamide at a molar ratio of chelate to protein of 5:1. After incubation for 20 h at 37°C, antibody–DTPA conjugates were purified using Biospin Column 6 (Bio-Rad) according to manufacturer's instructions.

For labeling antibody–DTPA conjugates with  $^{111}\text{In}$ ,  $^{111}\text{InCl}_3$  was incubated in 0.25 M acetate buffer (pH 5.5) for 5 min at room temperature, followed by incubation with antibody–DTPA conjugates for 1 h at 37°C. The labeled antibodies were purified using Biospin Column 6 (Bio-Rad). The radioactivity of the  $^{111}\text{In}$ -radioconjugates was measured using a gamma counter. The radiochemical purity of  $^{111}\text{In}$ -labeled MAb-6 ( $^{111}\text{In}$ -MAb-6) was more than 95%. The immunoreactivity of the antibody was maintained even after conjugation as determined by FACS.

For labeling antibody–DTPA conjugates with  $^{90}\text{Y}$ ,  $^{90}\text{Y}$  solution was incubated in acetate buffer (pH 5.5) for 5 min at room temperature, followed by incubation with antibody–DTPA conjugates for 1 h at 37°C. The labeled antibody was purified using Biospin Column 6. The radioactivity of  $^{90}\text{Y}$ -radioconjugates was measured using a curie meter.

#### Animal studies

The care and treatment of animals was in accordance with the guidelines of the Animal Care Committee of Gunma University (Gunma, Japan). Female BALB/c nude mice (age, 3–5 weeks; weight, 17–25 g) were purchased from Charles River Laboratories Inc. (Yokohama, Japan). Animals were inoculated intradermally in the right flank with 100  $\mu\text{l}$  (approximately  $1 \times 10^7$  cells) of A549, EBC1, H1373, RKO, or SW948 cells. Tumors were transplanted serially into nude mice by implanting tumor fragments measuring  $2 \times 2 \times 2$  mm. When tumors reached a mean size of 100–500  $\text{mm}^3$ , animals were randomly assigned to different groups.

#### Biodistribution study

Female nude mice inoculated with the tumors were selected (3 mice per group).  $^{111}\text{In}$ -MAb-6 and  $^{111}\text{In}$ -non-specific mouse IgG1 ( $^{111}\text{In}$ -mouse IgG) were injected intravenously

through the lateral tail vein. At 3, 24, and 48 h after injection, the animals were killed. Various tissues were collected and weighed, and the radioactivity of each tissue was determined using a gamma counter. The results of the distribution were expressed as the percentage of injected dose per gram of tissue (% dose/g) [19].

#### Therapeutic study

Mice with established tumors, i.e., EBC1, H1373, and SW948, were randomly divided into different treatment groups (6 mice per group). Mice were administered intravenous injections of PBS with 0.1% BSA, 20 µg of non-labeled MAb-6, 100 µCi of <sup>90</sup>Y-labeled MAb-6 (<sup>90</sup>Y-MAb-6, 20 µg), and 100 µCi of <sup>90</sup>Y-non-specific mouse IgG1 (<sup>90</sup>Y-mouse IgG, 20 µg). Mice were monitored for body weight and tumor volume. In EBC1 and SW948 tumor xenograft mouse models, 1 injection of <sup>90</sup>Y-MAb-6 was administered, while in H1373 tumor xenograft models, 2 injections were administered. In the latter, 100 µCi of <sup>90</sup>Y-MAb-6 was injected at 17 days after the first injection. Treated groups were observed until day 52. Tumor volume (mm<sup>3</sup>) was estimated by caliper measurement in 2 perpendicular directions and calculated using the following formula: (shortest diameter)<sup>2</sup> × (longest diameter) × 0.5 [19].

#### Histological analysis

Tissue specimens of H1373 tumor, heart, lung, liver, and kidney were obtained from mice at 7 days after injection. All samples were fixed in 10% neutral-buffered formalin overnight at 4°C. They were then embedded in paraffin and 5-µm sections were obtained. Slide sections were deparaffinized, dehydrated, and immersed in Mayer's Hematoxylin (Muto Pure Chemicals, Tokyo, Japan) and Eosin Y (Muto Pure Chemicals). Sections were treated with xylene and serially enclosed by Mount Quick (Daido Sangyo, Tokyo, Japan).

#### Statistical analysis

For the biodistribution study conducted using EBC1 tumor xenograft mouse models, the <sup>111</sup>In-MAb-6-treated group was compared with the <sup>111</sup>In-mouse IgG-treated group at 48 h after injection. Student's *t* test was performed, and *P* < 0.001 was considered statistically significant.

For evaluating biodistribution in lung tumor xenograft mouse models, the accumulation of <sup>111</sup>In-MAb-6 in EBC1 and H1373 tumors was compared with that in A549 tumors at 48 h after injection. In colorectal tumor xenograft models, the accumulation of <sup>111</sup>In-MAb-6 in SW948 tumors was compared with that in RKO tumors at 48 h after injection. Student's *t* test was performed, and *P* < 0.001 was considered statistically significant.

For therapeutic studies using EBC1, H1373, and SW948 tumor xenograft mouse models, the <sup>90</sup>Y-MAb-6-treated group was compared with the <sup>90</sup>Y-mouse IgG-treated group. Student's *t* test was performed for tumor volumes at day 28, and *P* < 0.01 was considered statistically significant. In the double-injection study of H1373 xenografts, the <sup>90</sup>Y-MAb-6 double-treated group was compared with the <sup>90</sup>Y-MAb-6 single-treated group at day 52.

## Results

### Establishment of MAb-6

We generated MAb-6 for the treatment for cancers expressing CDH3/P-cadherin. MAb-6 was generated by immunization with the expression vector designed to express a partial CDH3/P-cadherin protein corresponding to its extracellular domain. To examine the binding affinity of MAb-6 to the cell surface, we performed flow cytometry. MAb-6 was found to bind to the cell surfaces of the 3 CDH3/P-cadherin-expressing cell lines EBC1, H1373, and SW948 but not to those of the A549 and RKO cell lines, which showed no or very low CDH3/P-cadherin expression levels (Fig. 1a, b). We found a significant correlation between the mean fluorescent intensity (MFI) values of MAb-6 and expression levels of CDH3/P-cadherin molecules in these cell lines (Fig. 1b, c; *R*<sup>2</sup> = 0.95). In addition, we established cells that stably expressed CDH3/P-cadherin by transfecting either human or mouse CDH3/P-cadherin to the A549 cell line, in which CDH3 was not expressed. Furthermore, we performed flow cytometry to examine the specificity and cross-reactivity of MAb-6 with mouse CDH3. A high correlation between the MFI values of MAb-6 and expression levels of FLAG-tagged CDH3/P-cadherin was observed in all the transformed cell lines (Fig. 1d, e), suggesting that MAb-6 can specifically recognize native CDH3/P-cadherin and cross-react with mouse CDH3/P-cadherin. We also performed IHC analysis using anti-CDH3/P-cadherin monoclonal antibody (BD Transduction) to confirm CDH3/P-cadherin protein expression in normal human tissues. In accordance with the transcription levels observed, barely detectable levels of CDH3/P-cadherin protein were noted in the normal human heart, lung, liver, kidney, and pancreas; however, moderate levels were noted in the esophagus. By contrast, an upregulated and high expression level of CDH3/P-cadherin was observed in various cancer tissues (Supplementary Fig. 1, Table 1). Furthermore, CDH3/P-cadherin overexpression was observed in metastatic tissues, such as liver metastasis from colorectal cancer, lymph node, bone, and soft-tissue metastasis from lung cancer (Supplementary Fig. 2). Quantification of the expression level of CDH3/P-cadherin

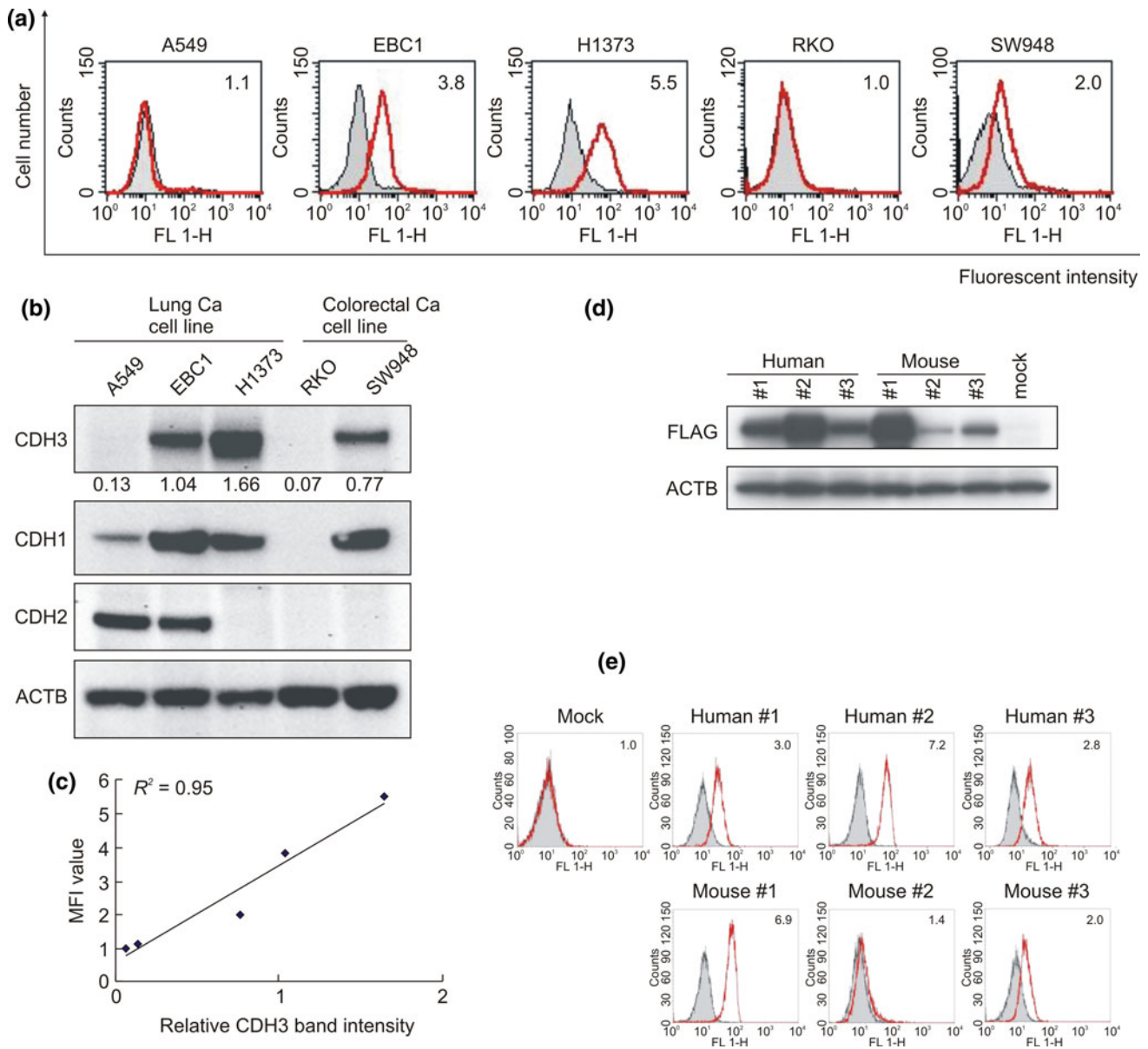


**Fig. 1** Establishment of MAb-6. **a** Immunoreactivity and specificity of MAb-6 by flow cytometry in 3 lung (A549, EBC1 and H1373) and 2 colorectal (RKO and SW948) cancer cell lines. The number within each panel indicates the MFI of MAb-6 against each cell line. *Red lines* indicate the fluorescent intensity incubated with MAb-6; *gray lines* indicate the fluorescent intensity incubated with non-immunized mouse IgG as a negative control. **b** Western blotting of CDH1, CDH2, and CDH3 protein expression in the lung and colorectal cancer cell lines. Cell lysates (30 µg) were loaded on the gel. ACTB served as a quantitative control. The relative CDH3 expression level was quanti-

fied and then normalized to the signal intensity of ACTB. **c** Correlation of CDH3 expression levels and MFI values of MAb-6 obtained from the data of A and B ( $R^2 = 0.95$ ). **d** Western blotting of cells expressing exogenous human and mouse CDH3 or those transfected with the mock vector. Exogenous induction of CDH3 expression was confirmed with anti-FLAG-tag mAb. ACTB served as the quantitative control. **e** Cross-reactivity of MAb-6 to mouse CDH3 protein. Flow cytometry was performed using MAb-6 in cells stably expressing human or mouse CDH3. The *numbers* in each histogram indicate the MFI values of each cell line

by immunohistochemical staining is a challenge for future studies.

**Distribution of MAb-6 in an in vivo model**

To evaluate the specificity of MAb-6 in vivo, we conducted a biodistribution study using nude mice with xenografted

tumors. Accumulation of  $^{111}\text{In}$ -MAb-6 in CDH3/P-cadherin-overexpressing EBC1 tumor increased throughout the experiments, from  $6.5 \pm 1.7\%$  dose/g at 3 h after injection to  $22.1 \pm 2.4\%$  at 48 h (Fig. 2a).

Tumor uptake of  $^{111}\text{In}$ -MAb-6 was significantly higher than that of  $^{111}\text{In}$ -mouse IgG ( $P < 0.001$ ; Fig. 2a). However, the uptake of  $^{111}\text{In}$ -MAb-6 in the blood, liver, kidney, intestine,

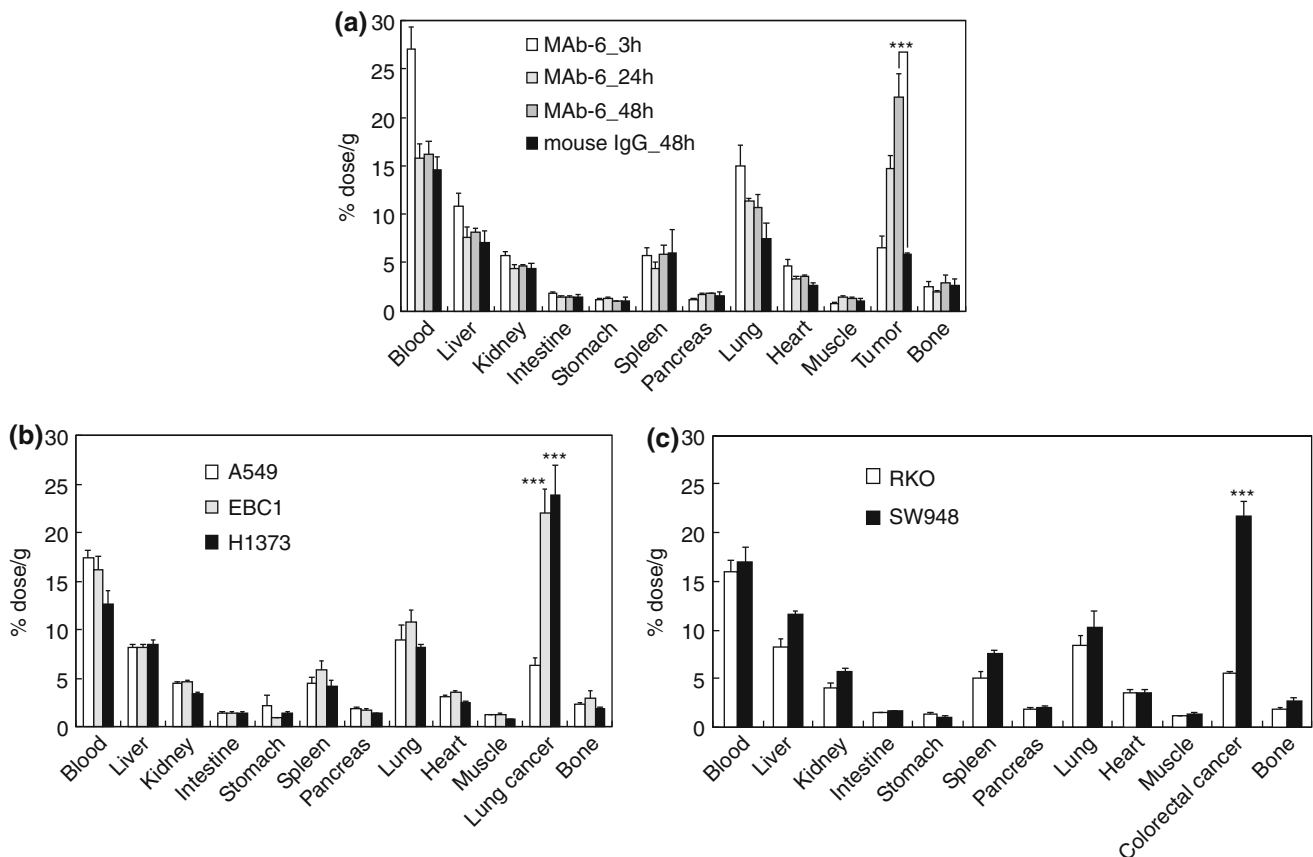


**Fig. 2** Biodistribution of MAB-6 in vivo. **a** Biodistribution of <sup>111</sup>In-MAB-6 and <sup>111</sup>In-mouse IgG in mice xenograft with EBC1 cells. DTPA-conjugated MAB-6 and normal mouse IgG were radiolabeled with <sup>111</sup>In and then injected intravenously into EBC1 tumor-inoculated mice. Mice injected with <sup>111</sup>In-MAB-6 were killed 3, 24, and 48 h after injection ( $n = 3/\text{group}$ ). The weight of blood, liver, kidney, intestine, stomach, spleen, pancreas, lung, heart, muscle, tumor, and bone tissues were evaluated. Mice injected with <sup>111</sup>In-mouse IgG were euthanized at 48 h after injection. Results represent the calculated percentages of the injected dose per gram of tissue (% dose/g). The <sup>111</sup>In-MAB-6-

treated group was compared with the <sup>111</sup>In-mouse IgG-treated group. Student's *t* test was performed, and  $P < 0.001$  was considered statistically significant. **b** Biodistribution of <sup>111</sup>In-MAB-6 in 3 lung tumor xenograft mouse models. Biodistribution was determined at 48 h after injection of <sup>111</sup>In-MAB-6 into mice with CDH3-positive (EBC1 and H1373) and CDH3-negative (A549) cells. **c** Biodistribution of <sup>111</sup>In-MAB-6 in 2 colorectal cancer xenograft mouse models. Biodistribution was determined at 48 h after injection of <sup>111</sup>In-MAB-6 in mice with CDH3-positive (SW948) and CDH3-negative (RKO) cells

stomach, spleen, pancreas, lung, heart, muscle, and bone remained constant or reduced gradually throughout the experiment (Fig. 2a). Furthermore, increased accumulation of <sup>111</sup>In-MAB-6 was observed in mice with CDH3/P-cadherin-overexpressing H1373, SW948, and EBC1 cells, but not in mice with CDH3/P-cadherin-negative A549 and RKO cells (Fig. 2b and c). However, CDH3/P-cadherin protein expression was detected in the normal esophagus; hence, we further examined the normal mouse esophagus in xenografted mouse models (Supplementary Fig. 1). We found no <sup>111</sup>In-MAB-6 accumulation in the esophagus (Supplementary Fig. 3a). Biotin–streptavidin IHC analysis confirmed that MAB-6 was specifically bound to the surface of cancer cells but not to that of normal esophageal cells at 48 h after injection (Supplementary Fig. 3b). These findings indicated that MAB-6 bound specifically to CDH3/

P-cadherin on the cell surface of the lung and colorectal cancers in vivo.

#### Antitumor effect of <sup>90</sup>Y-MAB-6 on CDH3-expressing xenografted tumors in nude mice

Although MAB-6 had no antitumor activity in vitro (data not shown), we designed RIT using <sup>90</sup>Y-MAB-6 for the treatment for cancers expressing CDH3/P-cadherin due to specific tumor accumulation of MAB-6. EBC1 (Fig. 3a), SW948 (Fig. 3b), and H1373 (Fig. 3c) cells were implanted in the flanks of BalB/c nude mice. When the mean size of tumors reached 100–500 mm<sup>3</sup>, <sup>90</sup>Y-MAB-6 (100 μCi), <sup>90</sup>Y-mouse IgG (100 μCi), non-labeled MAB-6, or PBS with 0.1% BSA were injected into mice intravenously. Tumors in non-labeled MAB-6- and PBS-treated mice grew

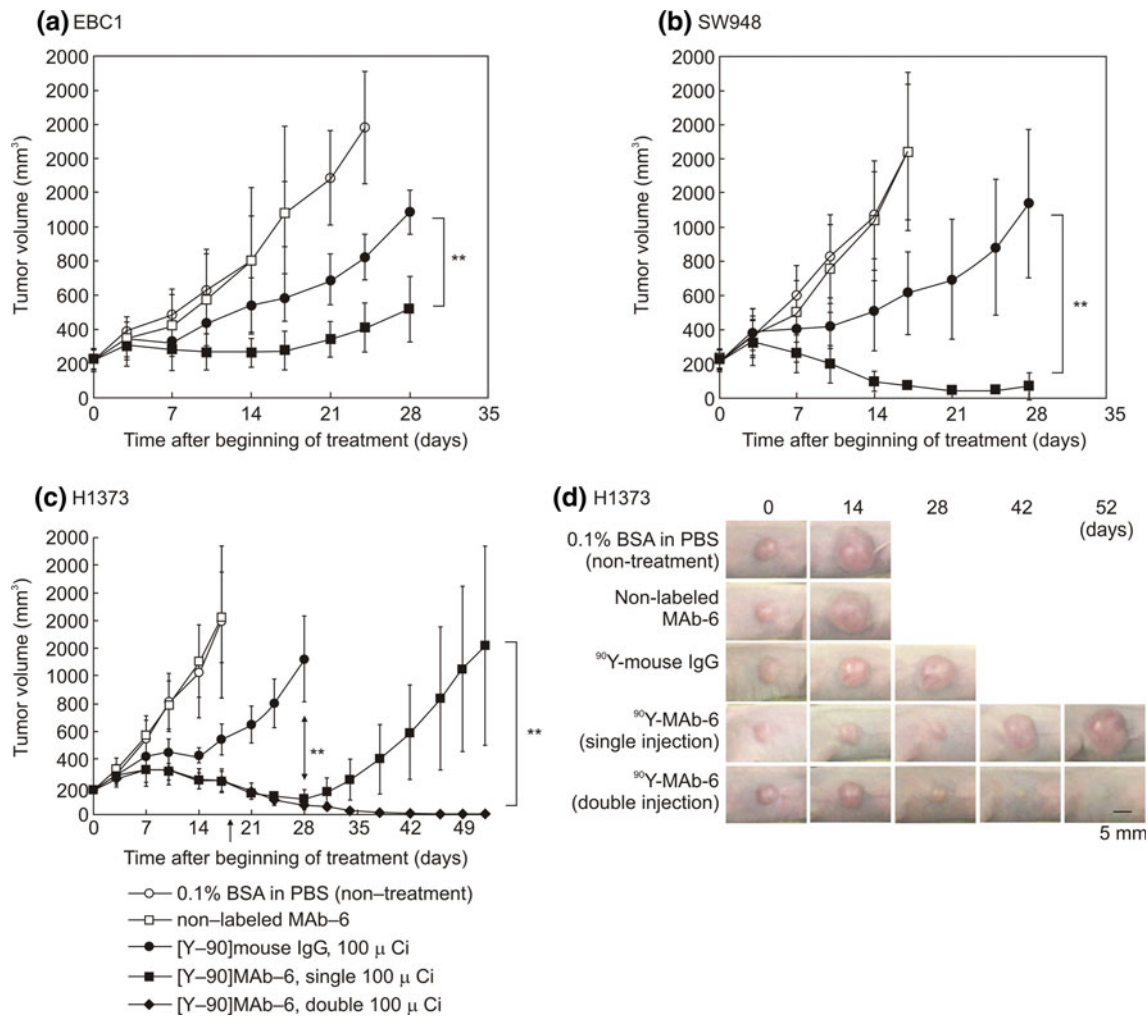


**Fig. 3** Antitumor effect of <sup>90</sup>Y-MAB-6 in mouse models using cells stably expressing CDH3. On day 0, mice with EBC1 (a), SW948 (b), and H1373 (c) cancer cell lines were assigned to the following groups: 0.1% BSA in PBS (non-treatment), non-labeled MAb-6, <sup>90</sup>Y-mouse IgG, and <sup>90</sup>Y-MAB-6 ( $n = 6/\text{group}$ ). <sup>90</sup>Y-MAB-6 and <sup>90</sup>Y-mouse IgG mice that revealed a similar specific radioactivity were injected intravenously at 100 μCi. Mice were monitored for tumor growth (tumor volume) over time. Student's *t* test was performed for tumor volumes on day 28, and  $P < 0.01$  was considered statistically significant. In the

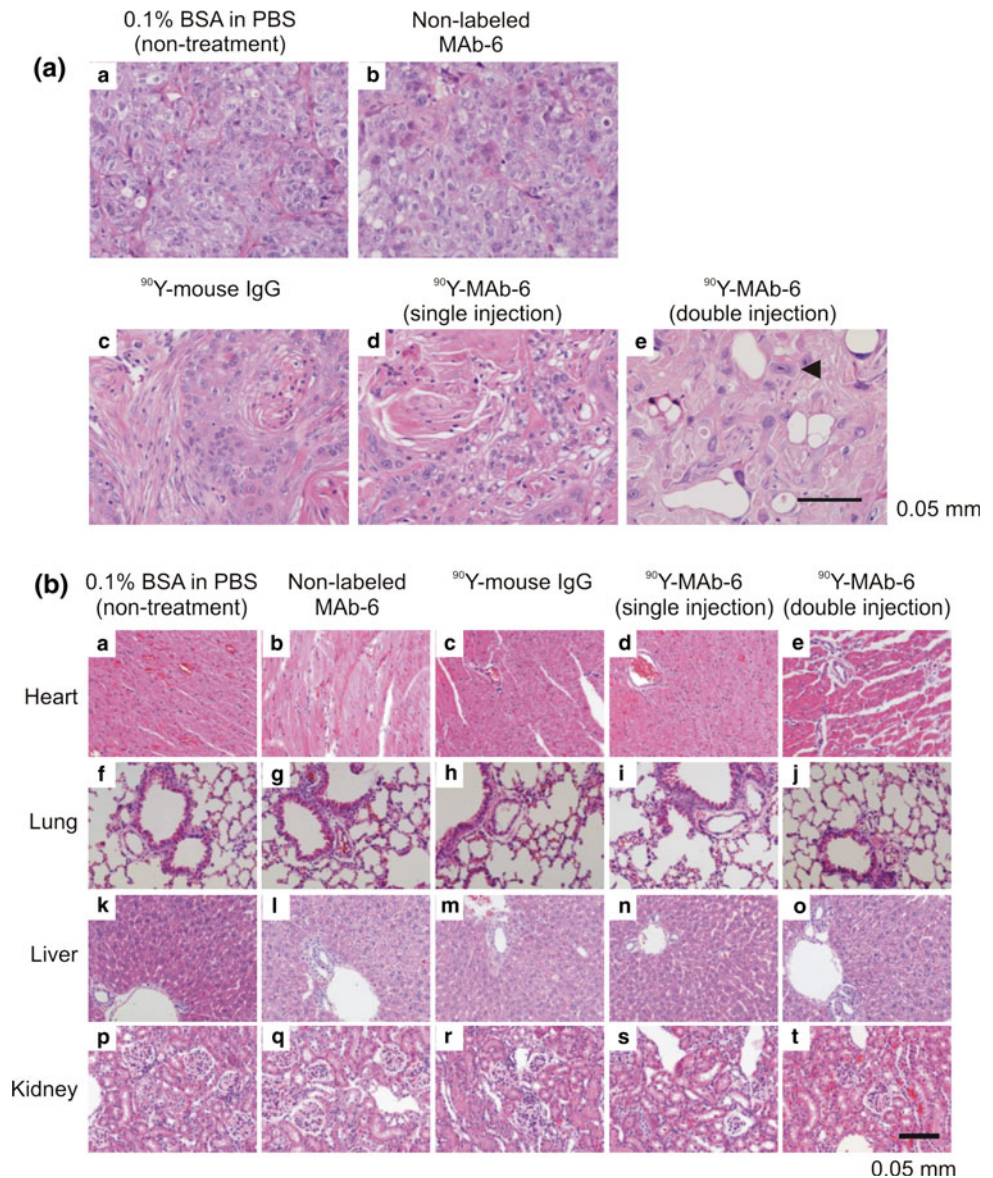
H1373 xenograft mouse models, <sup>90</sup>Y-MAB-6 was injected again at 17 days after the first injection. The <sup>90</sup>Y-MAB-6-treated group was compared with the <sup>90</sup>Y-mouse IgG-treated group. The <sup>90</sup>Y-MAB-6-treated group that was injected twice was compared with the <sup>90</sup>Y-MAB-6-treated group that was injected once on day 52. **d** Representative images of H1373 tumors treated with PBS, non-labeled MAb-6, <sup>90</sup>Y-mouse IgG, and <sup>90</sup>Y-MAB-6 (single and double injections). Photographs were taken on the days indicated. Scale bar = 5 mm

rapidly and exceeded a size of 1 cm<sup>3</sup> at day 14. However, in <sup>90</sup>Y-MAB-6-treated mice, tumor growth was significantly suppressed as compared to that in <sup>90</sup>Y-mouse IgG-treated mice at day 28 ( $P < 0.01$ ; paired *t* test, Fig. 3a–c). Importantly, repeated injections (day 0 and day 17) of <sup>90</sup>Y-MAB-6 resulted in the complete regression of tumors by day 52, although tumor regrowth was observed after day 28 in the mice that received a single injection (Fig. 3c, d).

We performed hematoxylin and eosin (H&E) staining using paraffin sections of resected tumors in H1373-inoculated mice at 7 days after the first or second injection of <sup>90</sup>Y-MAB-6, non-labeled MAb-6, <sup>90</sup>Y-mouse IgG, or PBS (Fig. 4a). No histological differences were observed in the

tumor tissues of non-labeled MAb-6- and PBS-treated mice. Fibrotic changes and a significant reduction in viable cancer cells were observed in the tumors of <sup>90</sup>Y-MAB-6-treated mice (single injection) but not in the tumors of <sup>90</sup>Y-mouse IgG-treated mice. In particular, the repeated injections of <sup>90</sup>Y-MAB-6 induced the abundant formation of giant nuclei in the tumor cells (Fig. 4a). However, no apparent histological changes were observed in the heart, lung, liver, or kidney tissues even 7 days after the second injection of <sup>90</sup>Y-MAB-6 (Fig. 4b). Mice that were injected with <sup>90</sup>Y-MAB-6 and <sup>90</sup>Y-mouse IgG showed a transient reduction in body weight, but this was corrected with baseline levels within 17 days; no additional detectable toxicity

**Fig. 4** Histological analysis of  $^{90}\text{Y}$ -MAB-6-treated mice. After injection, H1373 tumors (a) and normal tissues (b) (heart, lung, liver, and kidney) were excised on day 7. Tissues were paraffinized, cryosectioned, and stained with H&E. **a** The figure shows H1373 tumors in mice injected with PBS (a), non-labeled MAB-6 (b),  $^{90}\text{Y}$ -mouse IgG (c), and  $^{90}\text{Y}$ -MAB-6 [(d) single injection and (e) double injection]. Two injections of  $^{90}\text{Y}$ -MAB-6 resulted in abundant giant nuclei in cancer cells [(e) arrowhead, giant nucleus]. Scale bar = 0.05 mm. **b** The figure shows normal tissues in mice injected with PBS, non-labeled MAB-6,  $^{90}\text{Y}$ -mouse IgG, and  $^{90}\text{Y}$ -MAB-6. Heart (a–e), lung (f–j), liver (k–x), and kidney (o–y) tissues are shown from the top of the figure, respectively. Scale bar = 0.05 mm



was observed until 35 days after the second injection (Supplementary Fig. 4). Taken together, our results evidently indicate that the administration of  $^{90}\text{Y}$ -MAB-6 can be a potential strategy for the treatment for cancers that express CDH3/P-cadherin.

## Discussion

We have previously demonstrated that the antibody against CDH3/P-cadherin reduced the motility of cancer cells in vitro [17]. Therefore, we generated MAB-6 to establish a novel antibody-based anticancer therapy. We previously failed in several attempts to obtain CDH3/P-cadherin-specific mAbs through the use of recombinant proteins or peptides as antigens. This was probably

because of the native tertiary conformation of the CDH3/P-cadherin transmembrane glycoprotein. Therefore, in this study, we employed a genetic immunization method for the production of an antibody that would recognize the native conformation of CDH3/P-cadherin and successfully obtained MAB-6.

CDH3/P-cadherin belongs to the cadherin superfamily and is a single-span transmembrane glycoprotein that plays an important role in cell-to-cell adhesion [21–23]. The extracellular amino acid sequences of the CDH3/P-cadherin protein and propeptide sequences share 55 and 44% identity with those of CDH1/E-cadherin and CDH2/N-cadherin, respectively. In addition, human and mouse CDH3/P-cadherin share 85% identity. Hence, we investigated the cross-reactivity of MAB-6 with other members of the cadherin family. We found no cross-reactivity to CDH1/



E-cadherin or CDH2/N-cadherin; however, cross-reactivity to mouse CDH3/P-cadherin was observed.

When antibodies are employed for the treatment for human diseases, their immune reaction to normal tissues or cells often causes severe adverse reactions. When we investigated the *in vivo* distribution of MAb-6, we used radionuclide methods using an  $^{111}\text{In}$ -labeled antibody. We demonstrated that MAb-6 was bound to and accumulated in EBC1, H1373, and SW948 cells expressing CDH3/P-cadherin, whereas it did not bind to normal tissues or A549 and RKO cells that did not express CDH3/P-cadherin. In addition, although CDH3/P-cadherin protein expression was detected in the normal esophagus, we did not observe accumulation of MAb-6 in the esophagus of xenograft mice models or any detectable adverse reactions (except the temporary loss in body weight after injection of the radiolabeled antibody). The reason for antibody accumulation in tumors, but not in the normal esophagus, could be explained by the unique vascular characteristics of tumor tissue [24].

We have previously attempted to obtain anti-CDH3/P-cadherin antibodies with cytotoxic activities, such as antibody-dependent cell cytotoxicity, complement-dependent cytotoxicity, or apoptosis-inducing activity; however, these experiments have been unsuccessful thus far. However, in the course of these experiments, we observed effective internalization of the antibodies in cancer cells (data not shown); hence, we decided to employ  $^{90}\text{Y}$ -labeled antibodies for RIT in the treatment for cancer.  $^{90}\text{Y}$  emits radiation within a path length of 5 mm, and the effects of radiation are inversely proportional to the square of the distance from the radiation source. Radiation emitted from internalized radioisotopes has an increased probability of transversing the cells and interacting with the nucleus as compared to that emitted from surface-bound radioisotopes. Furthermore, we found that the antibody was degraded in the lysosomes following internalization. Chelated radiometals such as  $^{90}\text{Y}$  are known to move into the lysosomes [25–27], thereby increasing the retention time of  $^{90}\text{Y}$  and resulting in a greater therapeutic effect.

Our present study aimed to demonstrate the potential of CDH3/p-cadherin as a target of cancer therapy. Hence, we used within the maximum tolerated dose. In this study, although the body weight initially decreased after the injection of  $^{90}\text{Y}$ -labeled MAb-6, it later recovered completely.

Many researchers have reported data of blood count or H&E stain after injection of more than 100  $\mu\text{Ci}$  [28–30]. Especially, Sharkey et al. [28] have reported the data of blood count after injection to be 120  $\mu\text{Ci}$  of  $^{90}\text{Y}$ -labeled antibody against colon-specific antigen-p antibodies (Mu-9). The value of % dose/g of  $^{111}\text{In}$ -labeled MAb-6 in the bone is comparable to that of  $^{111}\text{In}$ -labeled Mu-9. In reference to these reports, we can speculate that the toxicity of

$^{90}\text{Y}$ -labeled MAb-6 in our study is comparable to that of  $^{90}\text{Y}$ -labeled Mu-9.

Further, for future prospects, we propose to conduct toxicity studies in greater details, which will include performing dose escalation studies and investigation into the relationship between therapeutic effect and toxicity.

In 2003, two radioisotope-conjugated anti-CD20 mAbs [ $^{90}\text{Y}$ -ibritumomab tiuxetan (Zevalin) and  $^{131}\text{I}$ -tositumomab (Bexxar)] were approved by the US Food and Drug Administration for treatment for NHL [8, 9], thus improving its clinical outcomes. Our previous data using  $^{90}\text{Y}$ -labeled FZD10 mAb for the treatment for synovial sarcoma in nude mice also indicated some promise in cancer patients [19]. We consider that anti-CDH3/P-cadherin mAbs have the potential to be similarly utilized in anticancer therapy.

Zhang et al. recently reported the development of a novel humanized therapeutic mAb to antagonize P-cadherin-regulated cell–cell adhesion [31]. However, the use of  $^{90}\text{Y}$  has the advantage of an intrinsic cross-fire effect that may overcome the heterogeneous expression of cancer cells with regard to the antigen [5]. Hence, our RIT approach using  $^{90}\text{Y}$ -MAb-6 may have potential for treating cancers that express CDH3/P-cadherin.

In conclusion, our data strongly suggest that CDH3/P-cadherin-targeting RIT using  $^{90}\text{Y}$ -MAb-6 can be a potential strategy for the treatment for cancers that express CDH3/P-cadherin.

**Acknowledgments** We would like to thank Dr. Megumi Takayanagi for contributions to this project. This study was funded by Oncotherapy Science Inc.

**Conflict of interest** The authors declare that they have no conflicts of interest.

## References

1. Maloney DG, Grillo-López AJ, White CA et al (1997) IDEC-C2B8 (Rituximab) anti-CD20 monoclonal antibody therapy in patients with relapsed low-grade non-Hodgkin's lymphoma. *Blood* 90:2188–2195
2. McNeil C (1998) Herceptin raises its sights beyond advanced breast cancer. *J Natl Cancer Inst* 90:882–883
3. Chen HX, Gore-Langton RE, Cheson BD (2001) Clinical trials referral resource: current clinical trials of the anti-VEGF monoclonal antibody bevacizumab. *Oncology (Williston Park)* 15:1017, 1020, 1023–1026
4. Baselga J (2001) The EGFR as a target for anticancer therapy—focus on cetuximab. *Eur J Cancer* 37(Suppl 4):S16–S22
5. Grossbard ML, Press OW, Appelbaum FR, Bernstein ID, Nadler LM (1992) Monoclonal antibody-based therapies of leukemia and lymphoma. *Blood* 80:863–878
6. Palanca-Wessels MC, Press OW (2010) Improving the efficacy of radioimmunotherapy for non-Hodgkin lymphomas. *Cancer* 116:1126–1133
7. Jain M, Venkatraman G, Batra SK (2007) Optimization of radioimmunotherapy of solid tumors: biological impediments and their modulation. *Clin Cancer Res* 13:1374–1382

8. Bischof DA (2003) The role of nuclear medicine in the treatment of non-Hodgkin's lymphoma (NHL). *Leuk Lymphoma* 44(Suppl 4):S29–S36
9. Chinn P, Braslawsky G, White C, Hanna N (2003) Antibody therapy of non-Hodgkin's B-cell lymphoma. *Cancer Immunol Immunother* 52:257–280
10. Nakamura T, Furukawa Y, Nakagawa H et al (2004) Genome-wide cDNA microarray analysis of gene expression profiles in pancreatic cancers using populations of tumor cells and normal ductal epithelial cells selected for purity by laser microdissection. *Oncogene* 23:2385–2400
11. Hasegawa S, Furukawa Y, Li M et al (2002) Genome-wide analysis of gene expression in intestinal-type gastric cancers using a complementary DNA microarray representing 23, 040 genes. *Cancer Res* 62:7012–7017
12. Lin YM, Furukawa Y, Tsunoda T, Yue CT, Yang KC, Nakamura Y (2002) Molecular diagnosis of colorectal tumors by expression profiles of 50 genes expressed differentially in adenomas and carcinomas. *Oncogene* 21:4120–4128
13. Kikuchi T, Daigo Y, Katagiri T et al (2003) Expression profiles of non-small cell lung cancers on cDNA microarrays: identification of genes for prediction of lymph-node metastasis and sensitivity to anti-cancer drugs. *Oncogene* 22:2192–2205
14. Takata R, Katagiri T, Kanehira M et al (2005) Predicting response to methotrexate, vinblastine, doxorubicin, and cisplatin neoadjuvant chemotherapy for bladder cancers through genome-wide gene expression profiling. *Clin Cancer Res* 11:2625–2636
15. Imai K, Hirata S, Irie A et al (2008) Identification of a novel tumor-associated antigen, cadherin 3/P-cadherin, as a possible target for immunotherapy of pancreatic, gastric, and colorectal cancers. *Clin Cancer Res* 14:6487–6495
16. Paredes J, Correia AL, Ribeiro AS, Albergaria A, Milanezi F, Schmitt FC (2007) P-cadherin expression in breast cancer: a review. *Breast Cancer Res* 9:214
17. Taniuchi K, Nakagawa H, Hosokawa M et al (2005) Overexpressed P-cadherin/CDH3 promotes motility of pancreatic cancer cells by interacting with p120ctn and activating rho-family GTPases. *Cancer Res* 65:3092–3099
18. Tang DC, De Vit M, Johnston SA (1992) Genetic immunization is a simple method for eliciting an immune response. *Nature* 356:152–154
19. Fukukawa C, Hanaoka H, Nagayama S et al (2008) Radioimmunotherapy of human synovial sarcoma using a monoclonal antibody against FZD10. *Cancer Sci* 99:432–440
20. Chinn PC, Leonard JE, Rosenberg J, Hanna N, Anderson DR (1999) Preclinical evaluation of 90Y-labeled anti-CD20 monoclonal antibody for treatment of non-Hodgkin's lymphoma. *Int J Oncol* 15:1017–1025
21. Wheelock MJ, Johnson KR (2003) Cadherins as modulators of cellular phenotype. *Annu Rev Cell Dev Biol* 19:207–235
22. Takeichi M (1988) The cadherins: cell-cell adhesion molecules controlling animal morphogenesis. *Development* 102:639–655
23. Nose A, Takeichi M (1986) A novel cadherin cell adhesion molecule: its expression patterns associated with implantation and organogenesis of mouse embryos. *J Cell Biol* 103:2649–2658
24. Jain RK, Baxter LT (1988) Mechanisms of heterogeneous distribution of monoclonal antibodies and other macromolecules in tumors: significance of elevated interstitial pressure. *Cancer Res* 48:7022–7032
25. Motta-Hennessy C, Sharkey RM, Goldenberg DM (1990) Metabolism of indium-111-labeled murine monoclonal antibody in tumor and normal tissue of the athymic mouse. *J Nucl Med* 31:1510–1519
26. Duncan JR, Welch MJ (1993) Intracellular metabolism of indium-111-DTPA-labeled receptor targeted proteins. *J Nucl Med* 34:1728–1738
27. Franano FN, Edwards WB, Welch MJ, Duncan JR (1994) Metabolism of receptor targeted 111In-DTPA-glycoproteins: identification of 111In-DTPA-epsilon-lysine as the primary metabolic and excretory product. *Nucl Med Biol* 21:1023–1034
28. Sharkey RM, Blumenthal RD, Behr TM, Wong GY, Haywood L et al (1997) Selection of radioimmunoconjugates for the therapy of well-established or micrometastatic colon carcinoma. *Int J Cancer* 29:477–485
29. Behr TM, Sgouros G, Stabin MG, Béhé M, Angerstein C et al (1999) Studies on the red marrow dosimetry in radioimmunotherapy: an experimental investigation of factors influencing the radiation-induced myelotoxicity in therapy with  $\beta$ -,  $\alpha$  or  $\alpha$ /conversion electron-, or  $\alpha$ -emitters. *Clin Cancer Res* 5:3031s–3043s
30. Esteban JM, Hyams DM, Beatty BG, Merchant B, Beatty JD (1990) Radioimmunotherapy of human colon carcinomatous xenograft with 90Y-ZCE025 monoclonal antibody: toxicity and tumor phenotype studies. *Cancer Res* 50:989s–992s
31. Zhang CC, Yan Z, Zhang Q et al (2010) PF-03732010: a fully human monoclonal antibody against P-cadherin with antitumor and antimetastatic activity. *Clin Cancer Res* 16:5177–5188